

Circulating cytokines and angiogenic factors based signature associated with the relative dose intensity during treatment in patients with advanced hepatocellular carcinoma receiving lenvatinib

Atsushi Ono, Hiroshi Aikata, Masami Yamauchi, Kenichiro Kodama, Waka Ohishi, Takeshi Kishi, Kazuki Ohya, Yuji Teraoka, Mitsutaka Osawa, Hatsue Fujino, Takashi Nakahara, Eisuke Murakami, Daiki Miki, Tomokazu Kawaoka, Hiromi Abe-Chayama, Peiyi Zhang, Songyao Liu, Grace Naswa Makokha, Masataka Tsuge, Michio Imamura, C. Nelson Hayes and Kazuaki Chayama

Abstract

Background: Although lenvatinib was recently approved for treatment of advanced unresectable hepatocellular carcinoma (HCC) based on the phase III REFLECT trial, no biomarkers for management of lenvatinib treatment have been established. The aim of this study is to identify predictive biomarkers for the management of lenvatinib treatment in advanced HCC patients.

Methods: A total of 41 patients with advanced HCC were enrolled in this retrospective study. Serum levels of 22 circulating cytokines and angiogenic factors (CAFs) were measured by multiplex Luminex assay. Profiles of CAFs, clinical chemistry/hematology parameters, and clinical background were evaluated to explore biomarkers associated with clinical outcomes.

Results: Relative dose intensity (RDI) decreased significantly between weeks 1–2 and 3–4 ($p < 0.001$), and RDI during weeks 3–4 was a prominent indicator of progression-free survival (PFS). A signature based on baseline serum levels of nine CAFs associated with low RDI was identified. In a multivariate Cox regression analysis, patients with a favorable 9-CAFs signature [hazard ratio (HR) 0.42, 95% confidence interval (CI) 0.18–0.96, $p = 0.040$] had lower risk, and Child-Pugh grade B (HR 1.6, 95% CI 1.1–8.3, $p = 0.026$) and presence of macrovascular invasion (MVI; HR 2.9, 95% CI 1.0–8.3, $p = 0.045$) had higher risk of shorter PFS.

Conclusion: This study demonstrates that RDI is an important predictive factor for longer PFS during lenvatinib treatment. In this hypothesis-generating exploratory analysis, we report that a CAF-signature associated with adverse events and RDI could predict PFS, which might contribute to improved management of lenvatinib treatment in HCC patients.

Keywords: biomarker, cytokine angiogenic factors, HCC, lenvatinib, relative dose intensity

Received: 23 October 2019; revised manuscript accepted: 13 March 2020.

Introduction

Hepatocellular carcinoma (HCC) is one of the most common malignant tumors and a leading cause of cancer-related death worldwide.¹ Lenvatinib, a novel oral multikinase inhibitor that

targets vascular endothelial growth factor (VEGF) receptors 1–3, FGF receptors 1–4, PDGF receptor α , RET, and KIT3, was recently approved in Japan ahead of the rest of the world to treat unresectable HCC. Prior to the approval of lenvatinib,

Ther Adv Med Oncol

2020, Vol. 12: 1–22

DOI: 10.1177/
1758835920922051

© The Author(s), 2020.
Article reuse guidelines:
sagepub.com/journals-
permissions

Correspondence to:

Kazuaki Chayama
Department of
Gastroenterology and
Metabolism, Graduate
School of Biomedical
and Health Sciences,
Hiroshima University,
1-2-3 Kasumi, Minami-
ku, Hiroshima 734-8551,
Japan

Research Center
for Hepatology and
Gastroenterology,
Hiroshima University,
Hiroshima, Japan

Institute of Physical
and Chemical Research
(RIKEN) Center for
Integrative Medical
Sciences, Yokohama,
Japan
[chayama@hiroshima-u.
ac.jp](mailto:chayama@hiroshima-u.ac.jp)

Atsushi Ono
Hiroshi Aikata
Masami Yamauchi
Kenichiro Kodama
Kazuki Ohya
Yuji Teraoka
Mitsutaka Osawa
Hatsue Fujino
Takashi Nakahara
Eisuke Murakami
Daiki Miki
Tomokazu Kawaoka
Hiromi Abe-Chayama
Peiyi Zhang
Songyao Liu
Grace Naswa Makokha
Masataka Tsuge
Michio Imamura
C. Nelson Hayes

Department of
Gastroenterology and
Metabolism, Graduate
School of Biomedical
and Health Sciences,
Hiroshima University,
Hiroshima, Japan

Waka Ohishi
Department of Clinical
Studies, Radiation Effects
Research Foundation,
Hiroshima, Japan

Takeshi Kishi
Biosample Research
Center, Radiation Effects
Research Foundation,
Hiroshima, Japan

Institute of Physical
and Chemical Research
(RIKEN) Center for

sorafenib was the only standard systemic therapy for unresectable HCC since 2007 that had been proven to improve survival in the SHARP and Asia-Pacific trials.^{2,3} Approval of lenvatinib was based on an international, multicenter, randomized, open-label, non-inferiority trial (REFLECT; [ClinicalTrials.gov identifier: NCT01761266]) that enrolled 954 patients with previously untreated, metastatic, or unresectable HCC. REFLECT demonstrated a statistically significant improvement in progression-free survival (PFS) with lenvatinib compared with sorafenib. Median PFS was 7.3 months in the lenvatinib arm and 3.6 months in the sorafenib arm (HR 0.64; 95% CI: 0.55, 0.75; $p < 0.001$) per modified response evaluation criteria in solid tumors (mRECIST); findings were similar according to RECIST 1.1. The overall response rate was higher for the lenvatinib arm than the sorafenib arm (41% versus 12% per mRECIST and 19% versus 7% per RECIST 1.1).^{4,5} Based on these results, lenvatinib was approved for treatment of HCC in March 2018 in Japan. Subsequently, it was also approved for treatment of HCC by the Food and Drug Administration in the United States on 16 August 2018, in Europe on 23 August 2018, in South Korea on 4 September 2018, in China on 29 August 2018, and in Taiwan on 28 November 2018.⁶

In recent years, various therapeutic agents for advanced HCC have been developed. As not all patients respond well to, or are able to tolerate, these agents, it is important to predict the response to treatment in order to select the most effective treatment for each patient and prevent unnecessary adverse events.

Tahara *et al.* reported that low baseline angiopoietin-2 level and upregulated fibroblast growth factor 23 (FGF-23) after the start of treatment were associated with longer PFS in differentiated thyroid cancer treated by lenvatinib.⁷ However, prognostic and predictive biomarkers for lenvatinib treatment of HCC have not been established to date.

The aim of the present study was to explore potential baseline predictive biomarkers of efficacy and relative dose intensity (RDI) in advanced HCC patients treated with lenvatinib from serum circulating cytokines and angiogenic factors (CAFs) and clinical parameters.

Maintaining high RDI during systemic therapy is important for the management of HCC.⁸ It was reported that maintaining an RDI $\geq 75\%$ during the initial 8 weeks of lenvatinib treatment had a favorable impact on response in a Japanese cohort.⁹ Stated differently, it is necessary to distinguish between patients with disease progression due to low biological response to lenvatinib and those due to low RDI.

We hypothesized that biomarkers associated with AFP decline in patients who maintain high RDI could act as surrogate markers for the biological response. Moreover, biomarkers associated with RDI might serve as surrogate markers for predicting a favorable impact on response, complementing markers of biological response.

Materials and methods

Patients

A total of 41 patients with advanced HCC who had started lenvatinib treatment at Hiroshima University Hospital between April and November 2018 were enrolled in this study. Collection of serum samples for this study was approved by the Hiroshima University ethical committee (approval numbers E-726-2 and HI-98, respectively) in accordance with the Declaration of Helsinki,¹⁰ and all patients provided written informed consent beforehand for the collection and use of data/samples for research and publication. The number of patients who underwent lenvatinib treatment during the enrollment period and provided informed consent determined the sample size. The inclusion criteria for treatment with lenvatinib were as follows: Child-Pugh liver function class A or B and an Eastern Cooperative Oncology Group performance status (ECOG PS) score of 1 or less, with two exceptions for patients whose PS were >1 according to a disease other than cancer. All patients satisfying the criteria were enrolled retrospectively without using stratification or matching. The end of follow up was January 2019, and the median follow-up period was 6.9 months. This study includes 32 patients with prior history of treatment with transcatheter arterial chemoembolization (TACE) or hepatic arterial infusion chemotherapy (HAIC), 18 patients with prior sorafenib treatment, and 10 patients previously treated with regorafenib (with some overlap). Adverse events were graded according

to the National Cancer Institute Common Terminology Criteria for Adverse Events version 4.0 (https://ctep.cancer.gov/protocoldevelopment/electronic_applications/ctc.htm).

Treatment regimens

Patients with a body weight of 60 kg or more started at a dose of 12 mg once a day, while the remaining patients started at a dose of 8 mg once a day (standard dose). Treatment interruptions and dose reductions were permitted in the case of adverse drug reactions. Patients continued therapy until death or until one of the following criteria was met for the cessation of therapy: disease progression, adverse events that required termination of treatment, deterioration of ECOG PS to 4, worsening liver function, or withdrawal of consent, with the exception of two patients who continued lenvatinib therapy after disease progression on the grounds that no other treatment option was available and lenvatinib was expected to slow disease progression more effectively than the best supportive care (BSC). After disease progression, 7 of the 31 patients underwent systemic post-lenvatinib treatments, 6 had non-systemic post-lenvatinib treatments, and 19 had BSC (Figure 1A).

Clinical and laboratory assessments

Clinical and laboratory assessments were performed before treatment. Serum α -fetoprotein (AFP) levels were also measured after 2 weeks of treatment. Objective response was evaluated by mRECIST after 4 weeks of treatment and every month subsequently.¹¹ Sera from all patients at baseline were aliquoted and stored at -80°C prior to serum protein profiling. For assessment of liver function, the albumin–bilirubin (ALBI) score was calculated using the following formula and used for grading (≤ -2.60 = grade 1, greater than -2.60 to ≤ -1.39 = grade 2, greater than -1.39 = grade 3): $\text{ALBI score} = [\log_{10} \text{bilirubin} (\mu\text{mol/l}) \times 0.66] + (\text{albumin (g/l)} \times (-0.0852))$.^{12,13} The primary endpoint of the study was PFS, and the secondary endpoint was overall survival (OS).

Assessment of profiles of circulating CAFs

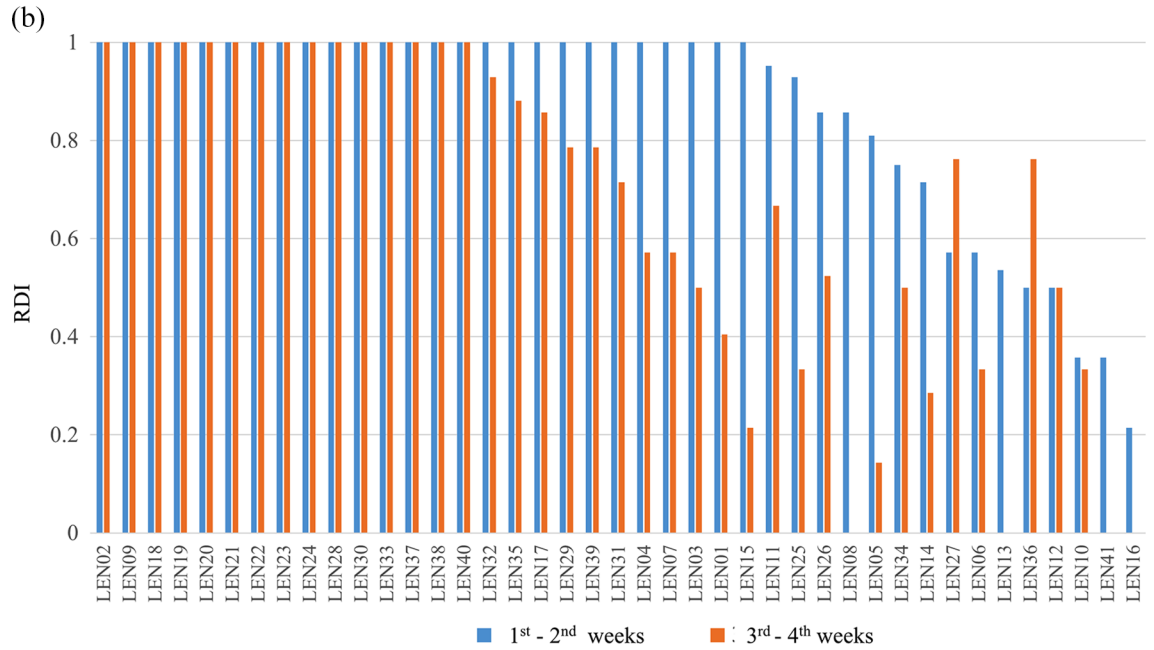
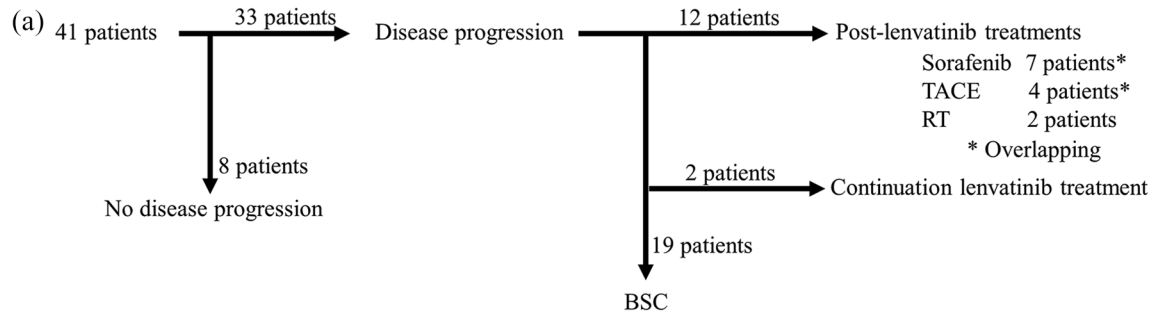
Multi-analyte profiling was performed for serum CAFs at baseline using the Human Luminex® Assay kit (R&D systems, Minneapolis, MN, USA) according to the manufacturer's instructions. The panel was designed by Luminex Assay

Customization Tool and consists of CAFs classified as plasma proteins, predicted secreted proteins and/or cancer-related proteins in the human protein atlas (<https://www.proteinatlas.org/>) and belonging to one or more of the following: BIOCARTEA, REACTOME, or KEGG (Kyoto Encyclopedia of Genes and Genomes) pathways associated with targets of lenvatinib: vascular endothelial growth factor receptor (VEGFR), fibroblast growth factor receptor (FGFR), platelet-derived growth factor (PDGF), the type III transmembrane receptor tyrosine kinase KIT, rearranged during transfection (RET), protein kinase B (AKT), and mitogen-activated protein kinase (MAPK) (<http://software.broadinstitute.org/gsea/msigdb>). In addition, proteins associated with Tie-2 signaling (REACTOME_TIE2_SIGNALING), which is one of the targets of regorafenib,^{14,15} proteins reported to be serum or plasma biomarkers for HCC,^{16–18} and proteins associated with tumor immunity,^{19–21} were also included in the panel. A summary of the panel design and the results of the Luminex assay are shown in Table S1. The assays were performed at Radiation Effects Research Foundation and were blinded with respect to patient characteristics and the study endpoint. The values below the lower end of the standard curve contained in the Luminex® Assay kit were treated as the values at the lower end of the standard curve. An assessment of the reliability of the assay is provided in a Supplemental document. The serum CAFs levels used in this analysis were obtained from one run in one plate to minimize confounding due to batch effects.

Statistical analysis

Intergroup differences between two groups of continuous or categorical variables were tested using the Mann–Whitney *U* test or the Fisher's exact test, respectively. Intergroup differences for 2×3 categorical variables were tested using the Chi-squared test. Comparison of the RDI between weeks 1–2 and 3–4 was assessed by paired *t* test. Inter-correlations of the serum levels of CAFs and clinical chemistry/hematology parameters were assessed by Pearson's correlation coefficient. These analyses were performed using JMP Pro14.0.0 (SAS Institute Inc., Cary, NC, USA). $p < 0.05$ was considered statistically significant.

The ComparativeMarkerSelection module was used to identify differences in serum protein



(c) Exploration of predictive biomarkers for

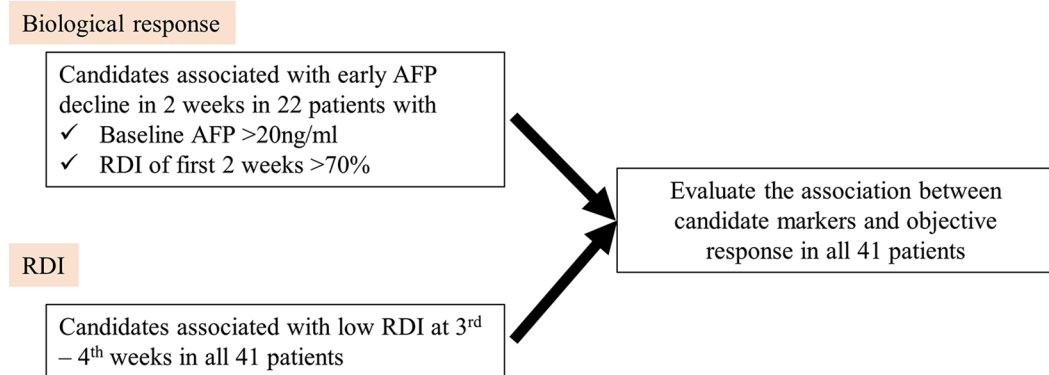


Figure 1. The concept and design of this study. (A) The flow of patients after disease progression. (B) Distributions of RDI: RDI during the 1st–2nd weeks (in blue) and the 3rd–4th weeks (in orange). (C) Strategy workflow for biomarker exploration. AFP, α -fetoprotein; BSC, best supportive care; RDI, relative dose intensity; RT, radiotherapy; TACE, transcatheter arterial chemoembolization.

Table 1. Patient characteristics.

Variables	<i>n</i> = 41
Age (years), median (range)	72 (46–84)
Sex (male/female), <i>n</i>	32/9
BW (kg), median (range)	59 (38–85.9)
≥60 kg/<60 kg	20/21
Dose (12 mg/8 mg), median (range)	22/19
TNM stage (I/II/III/IV/IVa), <i>n</i>	1/8/7/5/20
BCLC stage (B/C), <i>n</i>	13/28
Vp (yes/no)	6/35
Vv (yes/no)	3/38
MVI (yes/no)	7/34
Leukocyte count ($\times 10^4/\mu\text{l}$), median (range)	4700 (1470–10950)
Platelet count ($\times 10^4/\text{mm}^3$), median (range)	14.5 (4.2–39.4)
Albumin (g/dl), median (range)	3.3 (2.4–4.8)
PT (%), median (range)	80 (58–110)
Tbil (mg/dl), median (range)	0.8 (0.3–2.2)
AST (IU/l), median (range)	35 (14–214)
ALT (IU/l), median (range)	26 (9–107)
γ GTP (IU/l), median (range)	83 (11–716)
AFP (ng/ml), median (range)	1123 (0.5–2561000)
AFP-L3 (%), median (range)	25.2 (0–85)
DCP (AU/l), median (range)	1869 (16–418970)
Child Pugh grade (A/B), <i>n</i>	34/7
ALBI score	–2.06 [–1.06 to –3.37]
ALBI grade (1/2/3)	6/34/1
History of prior treatment (yes/no), <i>n</i>	
TACE	32/9
Sorafenib	18/23
Regorafenib	10/31
Etiology (presence/no), <i>n</i>	
HBV	7/34
HCV	9/32
HCV post SVR	9/32
Alcohol	6/35

AFP, alpha-fetoprotein; ALBI, albumin-bilirubin; ALT, alanine aminotransferase; AST, aspartate aminotransferase; BW, body weight; DCP, des-gamma-carboxy pro- thrombin; FT, free triiodothyronine; γ GTP, γ -glutamyl transpeptidase; HBV, hepatitis B virus; HCV, hepatitis C virus; PT, prothrombin time; SVR, sustained virologic response; TACE, transcatheter arterial chemoembolization.; TSH, thyroid-stimulating hormone.

Table 2. Patient characteristics of high and low RDI groups.

Parameter	High RDI	Low RDI	<i>p</i>
Age (years)	72 (46–83)	70 (57–84)	0.461
Sex (male/female)	19/4	13/5	0.471
Height (cm)	162.8 (151–176)	166 (151–174)	0.392
BW (kg)	59 (46–85.9)	71 (38–82.5)	0.906
Dose (12 mg/8 mg)	12/11	10/8	1.0
Leukocyte count ($\times 10^4/\mu\text{l}$)	4360 (1770–8680)	4065 (1470–10950)	0.160
Platelet count ($\times 10^4/\text{mm}^3$)	11.5 (4.9–31.1)	19.2 (4.2–39.4)	0.027
Albumin (g/dl)	3.4 (2.4–4.8)	3.1 (2.4–4.4)	0.023
PT-international normalized ratio (%)	81 (69–100)	77.5 (58–110)	0.674
Tbil (mg/dl)	0.8 (0.5–1.7)	0.9 (0.3–2.2)	0.315
AST (IU/l)	30 (17–86)	46 (14–214)	0.017
ALT (IU/l)	19 (10–69)	53 (9–107)	0.164
γ GTP (IU/l)	72 (11–192)	136.5 (15–716)	0.242
M2BPGi	2.82 (1.22–7.94)	4.225 (0.79–10.75)	0.131
ALIBI score	–0.37 (–0.51 to –0.15)	–0.30 (–0.61 to –0.03)	0.193
TSH ($\mu\text{IU/ml}$)	2.93 (0.8–23.8)	2.05 (1.07–17.3)	0.608
FT3 (pg/ml)	2.6 (2–3.3)	2.3 (1.6–3.4)	0.413
FT4 (ng/dl)	1.1 (0.8–1.4)	1.3 (0.8–1.5)	0.267
AFP (ng/ml)	480 (0.5–121590)	35069 (7.2–2561000)	0.101
AFP-L3 (%)	14.8 (0–85)	32.55 (5.2–79)	0.032
DCP (AU/l)	481 (16–108390)	155211 (25–418970)	0.006
Child Pugh grade (A/B)	21/2	13/5	0.209
ALBI score	–2.11 (–3.37 to –1.42)	–1.90 (–3.12 to –1.06)	0.033
TNM stage			
IVb/I-IVa	14/9	7/11	0.215
IV/I-III	10/13	6/12	0.540
III-IV/I-II	7/16	2/16	0.254
BCLC stage (B/C)	8/15	5/13	0.742
Vp (yes/no)	2/21	4/14	0.377
Vv (yes/no)	1/22	2/16	0.573
MVI (yes/no)	3/20	4/14	0.679

Table 2. (Continued)

Parameter	High RDI	Low RDI	<i>p</i>
Etiology			
HBV (yes/no)	2/21	5/13	0.209
HCV (yes/no)	6/17	3/15	0.706
HBV or HCV (yes/no)	8/15	7/11	1.0
History of prior treatment			
TACE (yes/no)	14/4	18/5	1.0
Sorafenib (yes/no)	12/6	6/17	0.013
Regorafenib (yes/no)	8/10	2/21	0.012
AFP, alpha-fetoprotein; ALBI, albumin-bilirubin; ALT, alanine aminotransferase; AST, aspartate aminotransferase; BCLC, Barcelona Clinic Liver Cancer; BW, body weight; DCP, des-gamma-carboxy pro- thrombin; FT, free triiodothyronine; γ GTP, γ -glutamyl transpeptidase; HBV, hepatitis B virus; HCV, hepatitis C virus; MVI, macrovascular invasion; PT, prothrombin time; TACE, transcatheter arterial chemoembolization; TSH, Thyroid-stimulating hormone; Vp, portal vein invasion; Vv, hepatic vein invasion.			

levels between the good and poor tolerability groups. Parameters were as follows: test statistic = 2-sided *t* test, number of permutations = 10,000. Development of a CAFs-based signature for categorizing low and high RDI groups with false discovery rate (FDR) < 0.05 was performed using the nearest template prediction (NTP) algorithm based on prediction confidence with FDR < 0.25.²² The reciprocal values of those nine proteins were used as the high RDI marker. The list of marker proteins is shown in Table S2. These analyses were performed using GenePattern (www.broadinstitute.org/genepattern).

Factors associated with cumulative PFS were assessed using Kaplan–Meier curves (for the entire follow-up period), log-rank test, and multivariate Cox regression hazard model. We used two models for the analysis exploring factors associated with PFS, early progressive disease (PD), and OS. Model 1 included the CAFs-based signature and the following factors that were reported by Hataoka *et al.* to be associated with PFS in HCC treated with lenvatinib²³: macrovascular invasion (MVI), extrahepatic metastasis, performance status. For model 2, the factors found to be associated with PFS or OS by the log-rank test were tested in the multivariate Cox regression hazard model using stepwise variable selection. Factors associated with early PD, defined as PD within 111 days, the median duration from the start of treatment to PD, were assessed using the Fisher's exact test. Factors

found to be associated with early PD and cumulative PFS were assessed using multivariate logistic regression.

The diagnostic values of CAFs for the stratification of RDI during the 3rd–4th weeks and the predictive values of CAFs for early PD were assessed using the area under the receiver operating characteristic (ROC) curve (AUC-ROC). We determined the threshold values using Youden's index. For continuous values, the median value was used as a threshold. Sensitivity, specificity, positive predictive value (PPV), and negative predictive value (NPV) were calculated for the assessment of the diagnostic utility of the 9-CAF signature and individual 9 CAFs using the cutoff mentioned above as predictors of RDI during 3rd–4th week and early PD.

There were no missing data in this study. The outcome assessment, recoding of the clinical data, and statistical analysis were performed by a different person in a blinded manner.

Definition

AFP decline was determined as follows: 1-(AFP level at 2 weeks/baseline AFP level). To suppress the influence of fluctuation in the normal range or low RDI, AFP decline was analyzed in patients with AFP levels of greater than 20 ng/ml at baseline and RDI > 70% in the first 2 weeks. Patients with AFP decline $\geq 30\%$ and < 30% were defined

as AFP decline and non-decline groups, respectively. RDI was calculated as follows: total dose of lenvatinib actually taken divided by the originally scheduled dose of lenvatinib during days 1–14 (weeks 1–2) and during days 15–28 (week 3–4). High and low RDI were classified as patients with RDI during weeks 3–4 of $\geq 70\%$ and $< 70\%$, respectively.

Results

Patient demographics and baseline characteristics are shown in Table 1. The median PFS time was 3.2 months [95% confidence interval (CI), 2.0–4.3]. Treatment-emergent adverse events of grade 3 or higher occurred in 14 patients. Hepatobiliary disorder, the most frequent grade 3 or higher adverse event, occurred in five patients.

Distribution of RDI

Figure 1B shows the distribution of RDI during weeks 1–2 and weeks 3–4. A paired *t* test revealed a significant decrease in RDI during weeks 3–4 compared with weeks 1–2 ($p < 0.001$).

Strategy work flow for exploration of biomarkers

From these results, we concluded that it was necessary to analyze biological response and tolerability separately. Therefore, we explored biomarker candidates associated with early AFP decline during the first 2 weeks as predictors of biological response. In a separate analysis, we examined candidates for biomarkers associated with low RDI (Figure 1C).

Prognostic role of AFP decline

First, we investigated early AFP response during the first 2 weeks as a marker of response to lenvatinib treatment. In order to suppress the influence of fluctuation in the normal range or low RDI, patients with baseline AFP levels < 20 ng/ml ($n = 11$) or with RDI $< 70\%$ ($n = 8$) during the first 2 weeks were excluded in this analysis. In the remaining 22 patients having AFP levels > 20 ng/ml at baseline and RDI $> 70\%$ during the first 2 weeks, AFP declines in patients with PD at 4 weeks were significantly smaller than those of patients with non-PD, including patients with either partial response (PR) or stable disease (SD) ($p = 0.02$) (Figure 2A). AFP declines in patients with mRECIST PR at 4 weeks were significantly

larger than those of patients with non-PR (PD or SD) ($p = 0.071$, respectively) (Figure 2B). The 11 patients who achieved AFP decline $> 30\%$ were defined as the AFP-decline group, and the other 11 patients were defined as the non-decline group, respectively. The median PFS in the AFP decline and non-decline groups were 6.7 months (95% CI, 2.2–13.2) and 3.5 months (95% CI, 1.0–4.0), respectively. Kaplan–Meier curves show longer PFS in the AFP-decline group than in the non-decline group ($p = 0.0081$) (Figure 2C).

Clinical characteristics and serum CAFs profile of the AFP decline and non-decline groups

Clinical characteristics of the AFP decline and non-decline groups are shown in Table S3. Albumin (Alb) levels ($p = 0.017$) were significantly higher and ALBI score ($p = 0.033$) was significantly lower in the AFP decline group. There was no CAF for which the level was significantly different between the AFP decline and non-decline groups (Table S4).

The distribution of AFP decline and objective response

The distribution of AFP decline in 22 patients with baseline AFP > 20 ng/ml and RDI $> 70\%$ during the first 2 weeks is shown in Figure 2D, which suggests that patients with PD at 4 weeks instead of AFP decline was due to low RDI, especially during weeks 3–4.

PFS according to RDI during the weeks 3–4

We defined patients with RDI $\geq 70\%$ during weeks 3–4 as the high RDI group, and patients with RDI $< 70\%$ as the low RDI group. The median PFS of the high and low RDI groups was 6.7 (95% CI, 3.9–9.9) and 2.6 (95% CI, 1.4–5.9) months, respectively. The PFS of the high RDI group was significantly longer than that of the low RDI group ($p = 0.011$) (Figure 2E).

Clinical characteristics of the high and low RDI groups

The clinical characteristics of the high and low RDI groups are shown in Table 2. Albumin levels were higher in the high RDI group. On the other hands, platelet count (Plt), alanine aminotransferase (ALT), AFP L3, and des-gamma-carboxy pro-thrombin (DCP) were higher in the low RDI group than in the high RDI group. Patients with a

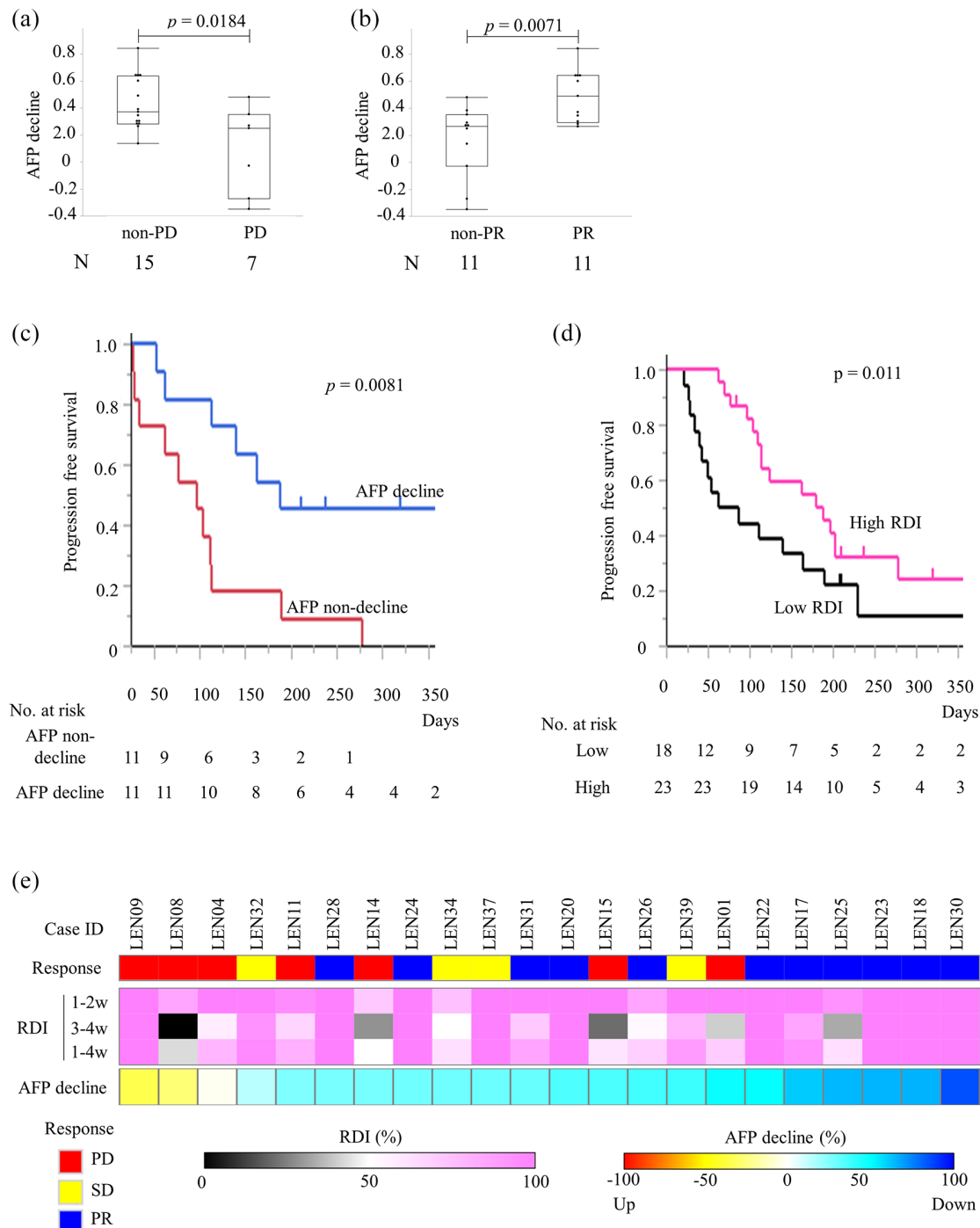


Figure 2. Prognostic role of AFP decline during the first 2 weeks and RDI during weeks 3–4. [A–C] Boxplot showing the distribution of AFP decline during the first 2 weeks in different objective response groups. Boxplots showing the distribution of AFP decline during the first 2 weeks. (A) Boxplot of AFP decline in patients with PD mRECIST response, and pooled patients with SD and PR (non-PD). (B) Boxplot of AFP decline in patients with partial mRECIST response (PR), and pooled patients with SD and PD (non-PR). (C) Kaplan–Meier estimates of PFS according to AFP decline: AFP-decline group (in blue) and AFP-non-decline group (in red). Patients who achieved AFP decline $\geq 30\%$ during the first 2 weeks were classified as the AFP decline group, and the others were defined as the AFP non-decline group. (D) The distribution of AFP decline. Upper boxes indicate the objective response of RECIST and mRECIST: PD (in red), SD (in yellow) and PR (in blue). The middle heatmap indicates RDI during the 1st–2nd weeks, 3rd–4th weeks, and 1st–4th weeks. The bottom heatmap indicates AFP decline during the first 2 weeks. (E) Kaplan–Meier estimates of PFS according to the RDI of 3rd–4th weeks. RDI rate of 3rd–4th weeks $\geq 70\%$ and $< 70\%$ were defined as the high (pink) and low (black) RDI groups. AFP, α -fetoprotein; PD, progressive disease; PR, partial response; PFS, progression-free survival; RDI, relative dose intensity; RECIST, response evaluation criteria in solid tumors; SD, stable disease.

Table 3. Diagnostic ability of CAFs and a 9-CAFs signature for stratification an RDI during 3rd–4th weeks.

		Cut-off (pg/ml)	AUROC	Specificity	Sensitivity	PPV	NPV
CAFs	VEGFR3	144.6	0.75	0.83	0.67	0.75	0.76
	FGF23	32.7	0.66	0.70	0.67	0.63	0.73
	FasL	46.1	0.74	0.57	0.94	0.63	0.93
	HGF	241.5	0.72	0.74	0.72	0.68	0.77
	VEGFD	305.9	0.62	0.96	0.44	0.90	0.69
	IL1R2	10135.7	0.73	0.96	0.56	0.91	0.73
	PDGF-BB	2613.8	0.77	0.61	0.89	0.64	0.88
	Neuropilin1	312895.2	0.74	0.70	0.72	0.65	0.76
	c-MET	140296.4	0.73	0.78	0.72	0.72	0.78
	9-CAFs signature	Non-favorable*			0.57	0.94	0.63
Unfavorable				0.91	0.61	0.85	0.75

AUROC, area under the ROC curve; CAFs, circulating cytokines and angiogenic factors; NPV, negative predictive value; PPV, positive predictive value.
*Unfavorable plus intermediate.

history of prior treatment with sorafenib or regorafenib were aggregated in the low RDI group.

Comparison of serum protein levels between the high and low RDI groups

The Comparative Marker Selection module (<http://software.broadinstitute.org>) was used to identify differences in serum CAF levels between the high and low RDI groups (Table S5). Scatterplots show the differential levels of serum CAFs between the high and low RDI groups (Figure 3A). Serum levels of IL-1 RII, VEGFR-3, c-MET, Neuropilin-1, PDGF-BB, FGF-23, HGF, VEGF-D, and FasL were significantly higher in the low RDI group (FDR < 0.05).

Serum CAFs-based signature associated with RDI

Signature-based categorization associated with high and low RDI was performed using the nine aforementioned CAFs. We named this signature the 9-CAFs signature. Figure 3B shows a heatmap visualization of the distribution of the 9-CAFs signature, serum levels of the CAFs composing the signature, RDI and objective response at 4 weeks, and adverse events. Incidence of

adverse events increased in a stepwise fashion among the favorable and unfavorable 9-CAFs signature groups (Figure 3C). A Kaplan–Meier curve shows the cumulative PFS and OS according to the 9-CAFs signature (Figure 4A and B, respectively). Median PFS of the patients with favorable, intermediate, and unfavorable signatures were 7.2 (4.0–13.0), 3.7 (1.9–7.0) and 3.1 (1.2–6.4) months, respectively. Patients with a favorable signature showed better PFS than patients with an unfavorable signature ($p = 0.026$). Median survival time (MST) of the patients with the favorable signature was not reached. MST of the patients with intermediate or unfavorable signature were 11.5 (4.8–NA) and 5.4 (1.3–9.1) months. A 9-CAFs signature significantly stratified the patients into the group with short, intermediate, or long MST ($p = 0.023$).

Diagnostic abilities of CAFs and a 9-CAFs signature for stratification of RDI during 3rd–4th weeks

AUROC, specificity, sensitivity, PPV, and NPV are shown in Table 3. In individual CAFs, PDGF-BB showed the highest AUROC (0.77). IL1-RII showed the highest specificity (0.96) and PPV (0.91) and FasL showed the highest sensitivity (0.94) and NPV (0.93). The ROC curves are shown

Table 4. Multivariate analysis associated with PFS early PD and OS (model 1).

Variable	PFS			Early PD			OS		
	HR	95% CI	<i>p</i>	OR	95% CI	<i>p</i>	HR	95% CI	<i>p</i>
9-CAFs signature									
Favorable	0.41	0.18–0.95	0.036	0.13	0.02–0.74	0.010			
Unfavorable							3.8	1.4–10.4	0.010
Extrahepatic metastasis									
Yes	1.3	0.61–2.6	0.533	0.7	0.17–3.0	0.63	1.6	0.6–4.3	0.337
MVI									
Yes	2.9	0.02–1.2	0.023	3.2	0.47–21.6	0.22	3.1	1.0–9.3	0.067
CAFs, circulating cytokines and angiogenic factors; MVI, macrovascular invasion; OS, overall survival; PD, progressive disease; PFS, progression-free survival.									

in Figure S1. The specificity, sensitivity, PPV, and NPV of the non-favorable (unfavorable plus intermediate) signature were 0.57, 0.94, 0.63, and 0.93, respectively. Those of the unfavorable signature were 0.91, 0.61, 0.85, and 0.75, respectively.

Factors associated with the outcome. The median PFS and OS of all patients were 5.0 and 11.0 months, respectively. PD was observed in 33 patients during the observation period. The median of the duration from the start of lenvatinib treatment to PD was 111 days in those patients. PD within 111 days was determined as early PD, and factors associated with early PD were assessed.

Model 1

Extrahepatic metastasis and MVI, which were reported to be associated with PFS in a recent report,²³ and the 9-CAFs signature were analyzed by multivariable analysis. From the results of Kaplan–Meier curve (Figure 4), the favorable and unfavorable signatures were used for analysis of PFS-/early PD- associated factors and OS associated factors, respectively.

Multivariate analysis of model 1 showed that 9-CAFs signature was an independent factor associated with PFS, OS, and early PD (Table 4).

Model 2

Factors associated with the cumulative incidence of PD. The following parameters were analyzed

by univariate analysis: age; sex; body weight (BW); leukocyte count; γ -glutamyl transpeptidase (γ GTP); prothrombin time (PT); Alb; total bilirubin (T-bil); aspartate aminotransferase (AST); ALT; Plt; M2BPGi; AFP; AFP-L3; DCP; portal vein invasion (Vp); hepatic vein invasion (Vv); MVI; Child-Pugh grade; prior treatment history; daily dose; tumour, node, metastasis (TNM) stage; Barcelona Clinic liver cancer (BCLC) stage; ALBI score; ALBI grade; and 9-CAFs signature. Parameters identified as factors associated with poor PFS were analyzed by multivariate analysis.

Univariate analysis identified the following pre-treatment factors associated with poor PFS: DCP (high, $p=0.034$), MVI (present, $p=0.001$), Child-Pugh grade (B, $p=0.017$), and 9-CAFs signature (favorable, $p=0.007$). Multiple Cox proportional hazard model analysis identified the favorable 9-CAFs signature (HR 0.42, 95% CI=0.18–0.96, $p=0.040$), MVI (HR 2.9, 95% CI=1.0–8.3, $p=0.045$) and Child-Pugh grade B (HR 3.1, 95% CI=1.1–8.3, $p=0.026$) as independent factors associated with poor PFS (Table 5).

Factors associated with early PD

The same parameters used for the analysis of factors associated with the cumulative incidence of PD were analyzed by univariate analysis.

The favorable 9-CAFs signature was identified as a factor associated with early PD by univariate analysis (OR=0.12, 95% CI=0.02–0.65, $p=0.010$).

Table 5. Prognostic factors for PFS.

Parameter	Univariate analysis	Multivariate analysis		
	<i>p</i>	Hazard ratio	95% CI	<i>p</i>
Age, high	0.741			
Sex, male	0.122			
BW, high	0.27			
Dose, 12 mg	0.091			
Leukocyte count, high	0.122			
γGTP, high	0.431			
PT, high	0.101			
Alb, high	0.075			
Tbil, high	0.074			
AST, high	0.122			
ALT, high	0.168			
Plt, high	0.553			
M2BPGi, high	0.104			
AFP, high	0.173			
AFP L3, high	0.917			
DCP, high	0.034	1.6	0.70–3.6	0.272
Child Pugh grade, BA	0.017	3.1	1.1–8.3	0.026
TNM stage				
IVb/I-IVa	0.896			
IV/I-III	0.7666			
III-IV/I-II	0.263			
BCLC stage (B/C)				
Vp (yes/no)	0.069			
Vv (yes/no)	0.097			
MVI (yes/no)	0.001	2.9	1.0–8.3	0.045
ALBI score, high	0.214			
ALBI grade, 2 or 3	0.348			
History of prior treatment				
TACE, yes	0.304			
Regorafenib, yes	0.164			
9-CAFs signature				
Favorable	0.007	0.42	0.18–0.96	0.04
Unfavorable	0.163			

The median was used as the cutoff for continuous values.

γGTP, γ-glutamyl transpeptidase; AFP, alpha-fetoprotein; ALBI, albumin-bilirubin; ALT, alanine aminotransferase; AST, aspartate aminotransferase; BCLC, Barcelona Clinic Liver Cancer; BW, body weight; DCP, des-gamma-carboxy pro- thrombin; FT3, free triiodothyronine; FT4, free thyroxine; HBV, hepatitis B virus; HCV, hepatitis C virus; MVI, macrovascular invasion; PT, prothrombin time; TACE, transcatheter arterial chemoembolization; TSH, thyroid-stimulating hormone; Vp, portal vein invasion; Vv, hepatic vein invasion.

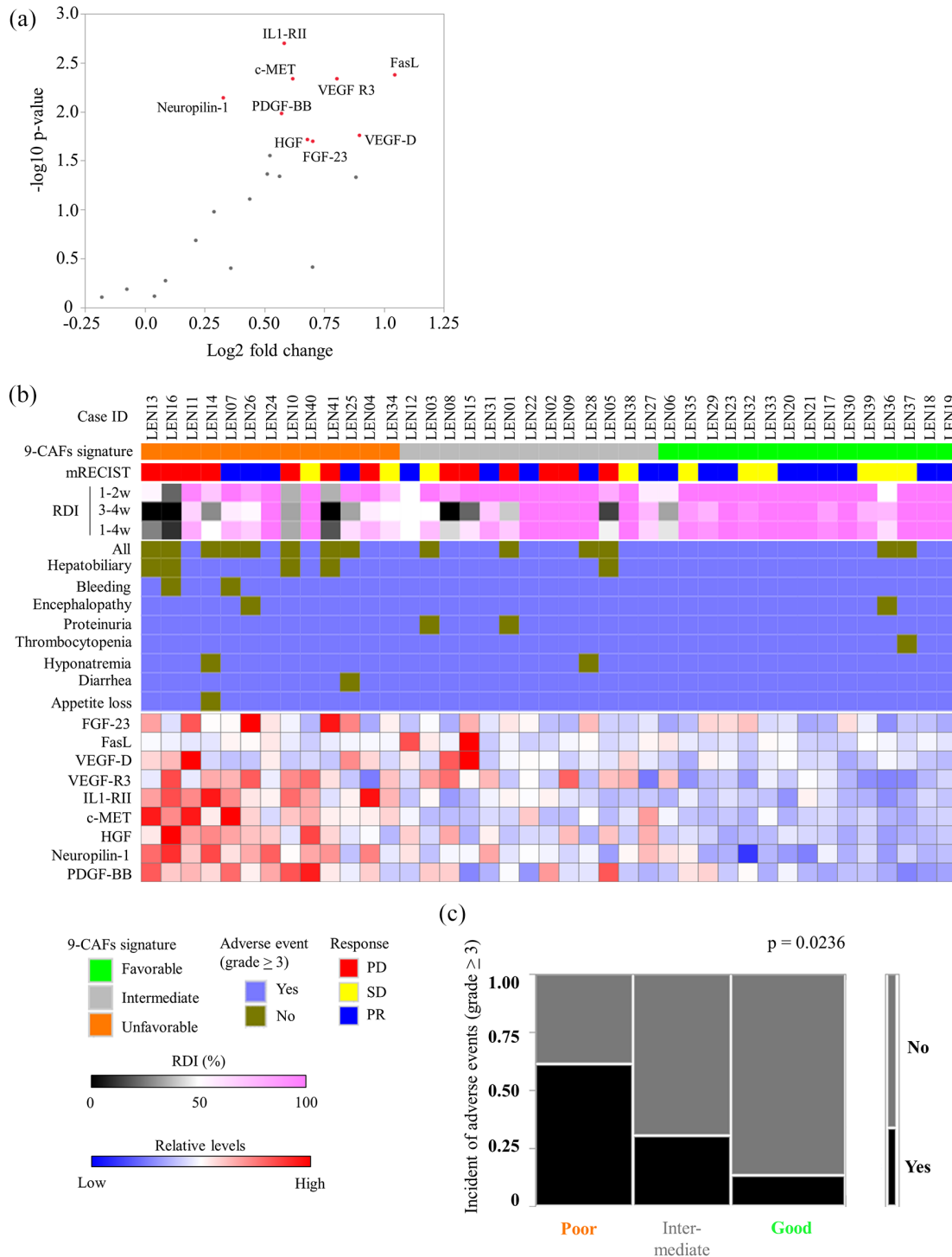


Figure 3. Serum CAF-based signature. (A) Scatterplots showing the differential levels of serum CAFs in the high and low RDI groups. The red dots indicate proteins with $\text{FDR} < 0.05$. (B) Heatmap showing the relative serum levels of 9-CAFs signature classification. The top rows indicate the classification according to 9-CAFs signature: favorable signature (light green), intermediate (gray), and unfavorable signature (orange). The second set of rows indicates the objective response of RECIST and mRECIST: PD (red), SD (yellow), and PR (blue). Pink-black heatmap indicating RDI during 1st–2nd weeks, 3rd–4th weeks, and 1st–4th weeks. The third set of boxes shows incidence of adverse events of grade ≥ 3 . The bottom heatmap indicates the relative serum levels of the component CAFs. (C) Mosaic plot showing the distribution of patients with adverse events of grade ≥ 3 according to the 9-CAFs signature. CAF, cytokine, angiogenic factor; FDR, false discovery rate; PD, progressive disease; PFS, progression-free survival; PR, partial response; RDI, relative dose intensity; RECIST, response evaluation criteria in solid tumors; SD, stable disease. p -values are based on the Chi-squared test.

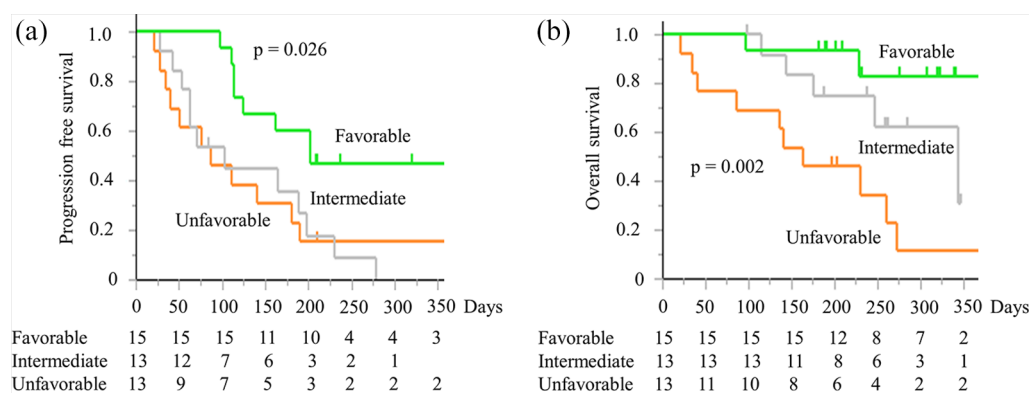


Figure 4. PFS and OS according to the 9-CAFs signature. Kaplan–Meier estimates of (A) PFS and (B) OS according to the 9-CAFs signature.

CAF, cytokine, angiogenic factor; OS, overall survival; PFS, progression-free survival.

Light green, gray, and orange lines indicate favorable, intermediate, and unfavorable signature, respectively.

The favorable 9-CAFs signature and factors associated with the cumulative incidence of PD (i.e. Child-Pugh grade and MVI) were assessed using multivariate logistic regression, which identified the favorable 9-CAFs signature as an independent predictor (OR=0.15, 95% CI=0.03–0.84, $p=0.032$) (Table 6).

Factors associated with OS

The same parameters used for the analysis of factors associated with the cumulative incidence of death were analyzed by univariate analysis. Univariate analysis identified the following pre-treatment factors associated with poor OS: γ GTP (high, $p=0.032$), T-bil (high, $p=0.004$), AST (high, $p=0.014$), M2BPGi (high, $p=0.015$), AFP (high, $p<0.001$), DCP (high, $p=0.010$), Child Pugh grade (B, $p<0.001$), ALBI score (high, $p=0.003$), Vp (presence, $p=0.013$), MVI (presence, $p=0.011$), 9-CAFs signature (favorable, $p=0.011$; unfavorable, $p<0.001$). Multivariate analysis identified Child Pugh grade (B, $p=0.001$, OR=9.0, 95% CI=2.4–34.1) and MVI (present, $p=0.030$, OR=4.1, 95% CI=1.1–14.5) as independent predictors (Table 7).

Correlation analysis of 9-CAFs signature composing factors and clinical parameters

Figure 5A and B show correlation coefficients and p -values of signatures composing CAFs and clinical chemistry/hematology parameters, respectively. Significant correlations ($|r| > 0.4$, $p < 0.05$) between the following CAFs and clinical chemistry/hematology parameters were observed:

IL1-RII, and c-MET were positively correlated with AST, ALT, and Plt. HGF and PDGF-BB were positively correlated with leukocyte count, AST, ALT, and Plt. Neuropilin-1 was positively correlated with AST and ALT, and negatively correlated with Alb. These results suggest that the signature was composed of two clusters and FGF-23. One cluster includes c-MET, Neuropilin-1, PDGF-BB, VEGF-R3, IL1-RII, and HGF, while the other cluster contains FasL and VEGF-D. A bubble chart (Figure 5C) illustrates the relationships among platelet count, ALBI score, and PDGF-BB. The sizes of the bubbles are determined by the serum PDGF-BB level. There was no correlation between platelet count and PDGF-BB levels ($r=0.123$ and $p=0.445$).

Predictive abilities of CAFs and a 9-CAFs signature for early PD

Table 8 shows the predictive abilities of CAFs and the 9-CAFs signature for early PD. In individual CAFs, Neuropilin-1 showed the highest specificity (1.0) and PPV (1.0), and PDGF-BB showed the highest AUROC (0.72) and NPV (0.81). The ROC curves are shown in Figure S2. The specificity, sensitivity, PPV, and NPV of the non-favorable (unfavorable plus intermediate) signature were 0.52, 0.88, 0.58, and 0.86, respectively. Those of the unfavorable signature were 0.78, 0.47, 0.62, and 0.67, respectively.

Discussion

The present study revealed that it is important to maintain high RDI during management of

Table 6. Prognostic factors for early progressive disease.

Parameter	Univariate analysis			Multivariate analysis		
	OR	95% CI	<i>p</i>	OR	95% CI	<i>p</i>
Age, high	1.4	0.39–5.1	0.747			
Sex, male	7.5	0.66–28.6	0.0605			
BW, high	1.0	0.28–3.5	1			
Dose, 8mg	1.4	0.39–5.0	0.748			
Leukocyte count, high	3.1	0.81–11.7	0.117			
γGTP, high	1.0	0.28–3.5	1.0			
PT, low	2.6	0.70–9.5	0.199			
Alb, low	2.8	0.75–10.3	0.197			
Tbil, high	4.3	0.98–19.2	0.056			
AST, high	1.3	0.36–4.6	0.755			
ALT, high	1.3	0.36–4.6	0.755			
Plt, high	3.1	0.81–11.7	0.117			
M2BPGi, high	0.66	0.18–2.4	0.748			
AFP, high	2.0	0.54–7.2	0.349			
AFP L3, high	0.56	0.15–2.0	0.52			
DCP, high	3.1	0.81–11.7	0.117			
Child Pugh grade, B	5.0	0.83–30.0	0.0942	1.4	0.39–5.2	0.592
TNM stage						
IVb/I-IVa	1.0	0.28–3.5	1.0			
IV/I-III	1.0	0.46–2.2	1.0			
III-IV/I-II	0.6	0.13–2.9	0.691			
BCLC stage (C/B)	0.91	0.23–3.6	1.0			
Vp (yes/no)	1.6	0.28–9.2	0.668			
Vv (yes/no)	0.73	0.06–8.8	1.0			
MVI (yes/no)	2.3	0.44–12.2	0.407	1.5	0.40–5.4	0.560
ALBI score, high	2.3	0.64–8.5	0.333			
ALBI grade, 2 or 3	3.9	0.42–37.5	0.373			
History of prior treatment						
Sorafenib, yes	3.3	0.89–12.5	0.106			
Regorafenib, yes	3.0	0.69–13.1	0.159			
9-CAFs signature						
Favorable	0.12	0.02–0.65	0.010	0.15	0.03–0.84	0.032
Unfavorable	2.3	0.6–9.0	0.305			

The median was used as the cutoff for continuous values.

γGTP, γ-glutamyl transpeptidase; AFP, alpha-fetoprotein; ALBI, albumin-bilirubin; ALT, alanine aminotransferase; AST, aspartate aminotransferase; BCLC, Barcelona Clinic liver cancer; BW, body weight; CI, confidence interval; DCP, des-gamma-carboxy pro-thrombin; FT3, free triiodothyronine; FT4, free thyroxine; HBV, hepatitis B virus; HCV, hepatitis C virus; MVI, macrovascular invasion; OR, odds ratio; PT, prothrombin time; TACE, transcatheter arterial chemoembolization; TSH, thyroid-stimulating hormone; Vp, portal vein invasion; Vv, hepatic vein invasion.

Table 7. Prognostic factors for overall survival.

Parameter	Univariate analysis	Multivariate analysis		
	<i>p</i>	Hazard ratio	95% CI	<i>p</i>
Age (high/low)	0.447			
Sex (male/female)	0.343			
BW (high/low)	0.943			
Dose (8 mg/12 mg)	0.563			
Leukocyte count (high/low)	0.318			
γGTP (high/low)	0.0324			
PT (low/high)	0.206			
Alb (low/high)	0.0623			
Tbil (high/low)	0.0037	3.8	0.79–18.8	0.096
AST (high/low)	0.0138			
ALT (high/low)	0.154			
Plt (high/low)	0.638			
M2BPGi (high/low)	0.0154			
AFP (high/low)	0.0009	4.2	0.89–20.5	0.072
AFP L3 (high/low)	0.898			
DCP (high/low)	0.0102			
Child Pugh, grade (B/A)	0.0001	9	2.4–34.1	0.001
TNM stage				
IVb/I-IVa	0.582			
IV/I-III	0.398			
III-IV/I-II	0.86			
BCLC stage (C/B)	0.328			
Vp (yes/no)	0.013			
Vv (yes/no)	0.404			
MVI (yes/no)	0.011	4.1	1.1–14.5	0.03
ALBI score (high/low)	0.0031			
ALBI grade (2 or 3/1)	0.588			
History of prior treatment				
Sorafenib (yes/no)	0.459			
Regorafenib (yes/no)	0.91			
9-CAFs signature				
Favorable	0.0105			
Unfavorable	<0.001			

γGTP, γ-glutamyl transpeptidase; AFP, alpha-fetoprotein; ALBI, albumin-bilirubin; ALT, alanine aminotransferase; AST, aspartate aminotransferase; BCLC, Barcelona Clinic liver cancer; CI, confidence interval; DCP, des-gamma-carboxy pro- thrombin; FT, free triiodothyronine; HBV, hepatitis B virus; HCV, hepatitis C virus; PT, prothrombin time; TACE, transcatheter arterial chemoembolization; TSH, thyroid-stimulating hormone.

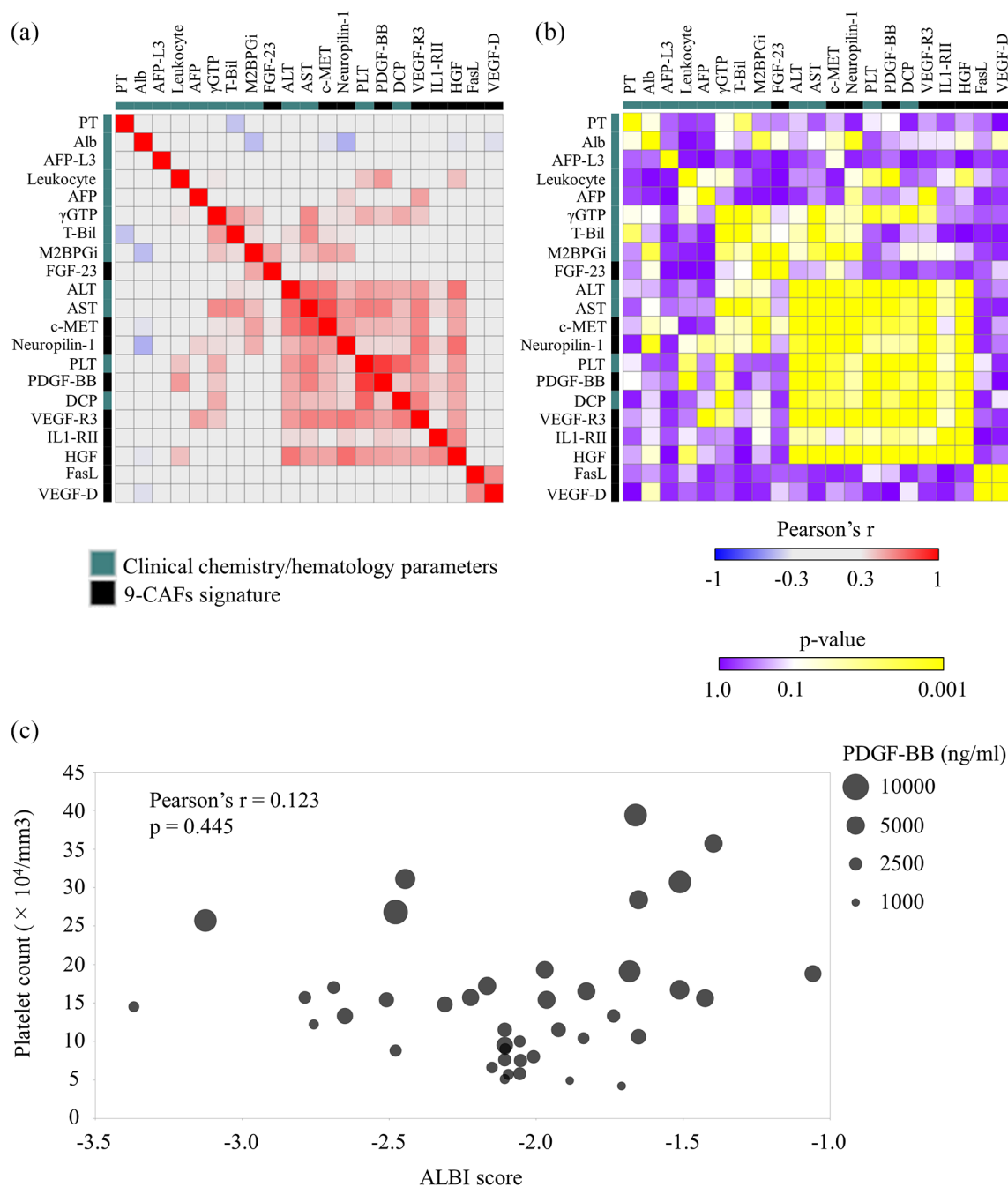


Figure 5. Correlation analysis of 9-CAFs signature composing factors and clinical parameters. Heatmap showing correlation coefficients (A) and p -values (B) of CAFs included in the signature with respect to clinical chemistry/hematology parameters. Green boxes indicate clinical chemistry/hematology parameters. Black boxes indicate the CAFs composing the signature. (C) Bubble chart showing the relationship of the platelet count, ALBI score, and PDGF-BB. The sizes of the bubbles are determined by the serum PDGF-BB level. ALBI, albumin-bilirubin; CAF, cytokine, angiogenic factor.

lenvatinib treatment in HCC patients. In particular, RDI after 3 weeks might be closely related to outcome, and we showed that RDI during the 3rd–4th weeks had a strong influence on PFS.

However, dosage reduction or discontinuation of treatment were required in 26 patients (63%) during this period, which means that predicting those patients who are likely to require dosage

Table 8. Predictive ability of CAFs and a 9-CAFs signature for early PD.

		Cut-off (pg/ml)	AUROC	Specificity	Sensitivity	PPV	NPV
CAFs	VEGFR3	210.0	0.64	0.87	0.41	0.70	0.67
	FGF23	32.7	0.57	0.61	0.59	0.53	0.67
	FasL	46.1	0.51	0.43	0.82	0.52	0.77
	HGF	294.7	0.64	0.74	0.59	0.63	0.71
	VEGFD	239.9	0.66	0.74	0.59	0.63	0.71
	IL1R2	8305.6	0.69	0.65	0.71	0.60	0.75
	PDGF-BB	3677.3	0.72	0.74	0.76	0.68	0.81
	Neuropilin1	412801.9	0.71	1.0	0.41	1.0	0.70
	c-MET	161793.0	0.50	0.74	0.41	0.54	0.63
9 CAFs signature	Non-favorable*			0.52	0.88	0.58	0.86
	Unfavorable			0.78	0.47	0.62	0.67

AUROC, area under the ROC curve; CAFs, circulating cytokines and angiogenic factors; NPV, negative predictive value; PD, progressive disease; PPV, positive predictive value.
*Unfavorable plus intermediate.

reduction or discontinuation is key to improving the treatment outcome by avoiding extreme lowering of RDI.

The low RDI group had higher levels of Plt, AST, and DCP and lower levels of Alb. The bubble chart (Figure 5C) suggests that Plt was positively correlated with PDGF-BB level independently from ALBI score. These results suggest that high Plt might be caused by HCC-driven dysregulation of CAFs rather than reflecting good liver function. We further identified a serum CAF signature associated with RDI during weeks 3–4, which we named the 9-CAFs signature. Incidence of adverse events with grade ≥ 3 , especially hepatobiliary disorder, was enriched with a worsening 9-CAFs signature. These findings suggest that the 9-CAFs signature could predict decreased RDI due to adverse effects.

Multiple Cox proportional hazard model analysis identified MVI in addition to the unfavorable 9-CAFs signature as factors associated with poor PFS. We previously reported that HAIC had a significantly better prognosis than sorafenib, a small molecule that inhibits tumor cell proliferation and tumor angiogenesis and whose inhibitory targets VEGFRs and PDGF- β are also primary targets of lenvatinib in patients with MVI and

non-TACE refractory HCC.^{2,24} These findings suggest that further investigation is needed to compare HAIC with lenvatinib therapy for HCC patients with MVI.

Multivariate logistic regression analysis of factors associated with early PD also showed an association between the unfavorable 9-CAFs signature and disease progression. We also assessed the predictive value of the 9-CAFs signature for early PD. The specificity/sensitivity of the non-favorable (unfavorable plus intermediate) signature and the unfavorable signature were 0.52/0.88 and 0.78/0.47, respectively (Table 8). Classifying the patients into three categories, including the intermediate group, is one of the characteristic points of the signature and enables it to handle intermediate levels appropriately depending on the situation; for example, the intermediate group will be included or excluded in the situation desiring high specificity or sensitivity, respectively (Table 8).

In other words, early management of treatment regimens, for example, scheduled withdrawal, might contribute to extend PFS in patients having unfavorable signatures. Treatment options for HCC have also broadened recently, and the signature might provide useful information to help

guide the choice of treatment or the right timing to switch to another regimen.

Although the 9-CAFs signature could stratify patients into groups with short, intermediate, or long MST, it was not identified as an independent factor associated with OS by multivariable analysis. The factors associated with OS identified by multivariable analysis were Child-Pugh grade and MVI. During the observation period, 21% and 18% of the patients underwent systemic and non-systemic post-levatinib therapy, respectively. Therefore, elements other than the factors associated with disease progression during levatinib treatment might affect OS.

A correlation matrix of CAFs and clinical chemistry/hematology parameters showed that signature-component CAFs formed two clusters. The larger cluster was inferred to be associated with pro-inflammatory state and included c-MET, neuropilin-1, PDGF-BB, IL1-RII, VEGF-R3, HGF with transaminase, and Plt.

The second cluster was composed of FasL and VEGF-D. Those two CAFs were not correlated with clinical chemistry/hematology parameters evaluated in the current study. FasL is a ligand of Fas, one of the so-called death receptors. After FasL engages with Fas, intracellular death domains interact with a number of adaptor proteins to trigger the apoptotic cascade. Convergence of apoptotic stimuli on the Fas signaling pathway likely promotes synergistic liver damage.²⁵ It has also been reported that exposure to environmental pollutants such as 2,3,7,8-tetrachlorodibenzo-p-dioxin increased NKT cell activation and exacerbated immune-mediated liver injury through a mechanism involving IFN γ and FasL expression.²⁶

Moreover, blockage of one pathway could cause upregulation of another pathway. For instance, it was reported that VEGFR2 inhibition upregulated ANG2 and vascular TIE2 and enhanced infiltration by TIE2-expressing macrophages in the PNETs.²⁷ Berkkanoglu *et al.* reported that FasL was downregulated by VEGF, and that anti-VEGF neutralizing antibody alone resulted in an increase in FasL expression in endometrial stromal cells.²⁸

At the same time, the CAF heatmap suggested that sphenia of multifocal pathways was occurring in patients with unfavorable CAFs-based signatures.

Based on those reports and results, we inferred that inhibition of specific angiogenesis and tumor fibroblast growth factor signaling pathways by levatinib induces upregulation of other pathways in patients in whom these signaling pathways were originally and multifocally upregulated, which could cause adverse events *via* mechanisms such as vascular hyperpermeability and death signal induction by FasL.^{25,29}

Exploratory analysis from a phase II trial for renal cell carcinoma (RCC), in which patients were randomized to levatinib, everolimus, or levatinib plus everolimus treatment groups, showed that baseline Ang2 and VEGF levels were prognostic but not predictive factors. Elevated baseline FGF-23 levels were associated with longer OS only in the levatinib group. However, none of these biomarkers were predictive of response to levatinib treatment alone or in combination.³⁰ An exploratory analysis of differentiated thyroid cancer showed that lower baseline Ang2 level and upregulation of FGF-23 after the start of treatment was associated with longer PFS in a subgroup of levatinib-treated patients.⁷

On the other hand, our analysis indicates that high baseline FGF23 level was one of the elements constituting a CAFs signature associated with low RDI and shorter PFS. We considered that it is important to consider the following two disease progression cases separately in our cohort; the cases owing to the lack of response to levatinib and those owing to the low RDI. In this study, we focused on the former because there were only a limited number of patients who maintained high RDI. Importantly, the tolerability and profile of the adverse events were different between HCC patients and other cancer patients. In fact, although the tolerable dose in patients with RCC and thyroid cancer is 24mg once daily,^{31,32} a phase I study of levatinib in HCC showed the maximum tolerable dose in patients with HCC and Child Pugh (CP) class A liver function was 12 mg once daily.³³ Finally the starting dose of levatinib was adopted as 12mg for patients ≥ 60 kg and 8 mg for patients < 60 kg once-daily depending on BW and pharmacokinetic modelling data.

Although an elevated AST and increased blood bilirubin (any grade/grade > 3 were 14/5 and 15/7%, respectively) were reported in a phase III trial in HCC,⁵ these events were not observed in

clinical trials of RCC and thyroid cancer.^{31,32} The heatmap (Figure 3B) shows that the hepatobiliary disorder events were more common in patients with the aforementioned unfavorable CAFs signature, and these were the most common events causing low RDI. Those differences could cause the discrepancy between our results and those of previous findings in studies in RCC or thyroid cancer patients.

Recently, a synergistic effect of immune checkpoint blockade and anti-angiogenesis in cancer treatment has been attracting attention, and a lot of clinical trials investigating the efficacy of ICI plus anti-angiogenesis therapy are ongoing.^{34,35} Tumor angiogenesis tilts the tumor microenvironment towards an immunosuppressive state in solid cancers.

Several mechanisms have been advanced, as follows: (1) high interstitial fluid pressure induced by leaky nascent vessels and loose pericyte coverage causes a greater pressure difference for T cell infiltration to overcome. (2) The lack of certain adhesion molecules observed in nascent vessels, such as vasculature cell adhesion molecule-1 (VCAM-1), impairs T cell extravasation. (3) Several immune inhibitory signals such as PD-L1, indoleamine 2, 3-dioxygenase (IDO), interleukin-6 (IL-6), interleukin-10 (IL-10) and chemokine (C-C motif) ligand-22 and chemokine (C-C motif) ligand-28 are upregulated by hypoxia. (4) Circulating VEGF inhibits the maturation and function of dendritic cells (DCs). (5) The polarization of tumor-associated macrophages (TAM) to the M2/pro-tumour phenotype is promoted by the hypoxic tumor microenvironment. (6) The FasL on tumor endothelial barrier selectively impedes infiltration of CD8+ T cells rather than Treg.³⁴ ANGPTL4 (angiopoietin-like protein 4), a member of the angiopoietin-related family, was previously reported to play a crucial role in regulating angiogenesis and glucolipid metabolism.^{36,37} Recently, Nie *et al.* reported that upregulation of ANGPTL4 was associated with advanced tumor stage, deep stromal invasion, lymph node metastasis, lymphovascular space invasion, as well as poor OS and DFS in cervical cancer.³⁷ Moreover, Argentiero *et al.* reported that Angiopoietin-like 4 (ANGPTL4), which is involved in regulation of immune homeostasis, modulating inflammatory T cell response, and expression of several cytokines, such as IL10 and IL1, was related to angiogenesis and tumor migration *via* $\alpha 5\beta 1$ -integrin/RAC1 interaction in pancreatic cancer.³⁸

These findings suggest that angiogenesis factors have a beneficial role in survival, growth, or spread of cancer. Therefore, anti-angiogenic agents such as lenvatinib are expected to be particularly effective in patients in whom angiogenesis is upregulated. However, the present study revealed that patients with high CAFs were associated with low RDI due to adverse events. A task for the future is to manage lenvatinib treatment well in these patients in order to maintain high RDI.

The present study demonstrated that it is necessary to consider biological response and RDI separately to explore biomarkers for lenvatinib treatment in advanced HCC patients. We analyzed the decline of AFP during the first 2 weeks rather than the first 4 weeks because the number of patients with RDI > 70% during the first 4 weeks was only 26 in contrast with the 33 patients who experienced RDI > 70% during the first 2 weeks. Although the baseline serum Alb level was significantly higher in the AFP decline group, no other suitable candidates for predicting AFP decline were found in these 22 patients. Further analysis with more patients or using other biomarkers is necessary to explore biomarkers for the biological response to lenvatinib.

The median PFS and OS were 5.0 and 11.0 months, which were shorter than those of 7.3 and 13.6 months reported in the REFLECT study.⁵ The shorter PFS and OS might be due to differences in the clinical background. Although patients were excluded if they had received previous systemic therapy for hepatocellular carcinoma in the REFLECT study, 18 out of 41 (44%) patients had received sorafenib, and 10 out of 18 patients had also received regorafenib. Median age was 63 and 72 years, and the proportions of patients with Child-Pugh class A was 99% and 83% in the REFLECT study and the current study, respectively.

The reproducibility of the findings of this study was confirmed by comparing the results obtained from a pilot study with those of the current analysis. Although there was some deviation in the values measured using the Luminex and ELISA assays in four randomly selected samples, the trends were maintained in HGF and FGF-23, consistent with the CAFs signature. Therefore, additional inspection will be necessary to use values measured by other modalities.

Although the small sample size and lack of a separate validation set are important limitations of this

study, and further prospective analysis is necessary to draw conclusions, considering that lenvatinib was only approved for HCC in 2018, we consider these early exploratory results to provide initial guidance with respect to the role of RDI in PFS and risk of adverse events in patients undergoing lenvatinib therapy.

Conclusion

This study demonstrates that RDI was a key factor for longer PFS. This hypothesis-generating exploratory biomarker analysis demonstrated that a CAFs signature associated with adverse events and RDI could predict clinical outcomes of lenvatinib treatment in patients with advanced HCC, which could contribute to better management of these patients.

Acknowledgments

The authors thank Akemi Sada, Emi Nishio, and Hitomi Sasaki for clerical assistance.

Conflict of interest statement

Kazuaki Chayama has received research funding from Eisai. The funder had no role in the design of the study, collection, analysis, interpretation of data, writing of the manuscript or decision to publish the results.

Funding

The authors disclosed receipt of the following financial support for the research, authorship, and/or publication of this article: This work was supported by Japan Society for the Promotion of Science (JSPS) KAKENHI (Grant Number 17K15948) and grants from Sumitomo Dainippon Pharma Co. (Grant Number DSPS20180524012).

Supplemental material

Supplemental material for this article is available online.

References

1. GBD 2016 Causes of Death Collaborators. Global, regional, and national age-sex specific mortality for 264 causes of death, 1980–2016: a systematic analysis for the global burden of disease study 2016. *Lancet* 2017; 390: 1151–1210.
2. Llovet JM, Ricci S, Mazzaferro V, *et al.* Sorafenib in advanced hepatocellular carcinoma. *N Engl J Med* 2008; 359: 378–90.
3. Cheng AL, Kang YK, Chen Z, *et al.* Efficacy and safety of sorafenib in patients in the Asia-Pacific region with advanced hepatocellular carcinoma: a phase III randomised, double-blind, placebo-controlled trial. *Lancet Oncol* 2009; 10: 25–34.
4. Kudo M. Lenvatinib may drastically change the treatment landscape of hepatocellular carcinoma. *Liver Cancer* 2018; 7: 1–19.
5. Kudo M, Finn RS, Qin S, *et al.* Lenvatinib versus sorafenib in first-line treatment of patients with unresectable hepatocellular carcinoma: a randomised phase 3 non-inferiority trial. *Lancet* 2018; 391: 1163–1173.
6. Kudo M. Targeted and immune therapies for hepatocellular carcinoma: predictions for 2019 and beyond. *World J Gastroenterol* 2019; 25: 789–807.
7. Tahara M, Schlumberger M, Elisei R, *et al.* Exploratory analysis of biomarkers associated with clinical outcomes from the study of lenvatinib in differentiated cancer of the thyroid. *Eur J Cancer* 2017; 75: 213–221.
8. Wang W, Tsuchiya K, Kurosaki M, *et al.* Sorafenib-Regorafenib sequential therapy in Japanese patients with unresectable hepatocellular carcinoma—relative dose intensity and post-regorafenib therapies in real world practice. *Cancers (Basel)*. Epub ahead of print 9 October 2019. DOI: 10.3390/cancers11101517.
9. Takahashi A, Moriguchi M, Seko Y, *et al.* Impact of relative dose intensity of early-phase lenvatinib treatment on therapeutic response in hepatocellular carcinoma. *Anticancer Res* 2019; 39: 5149–5156.
10. World Medical Association. World medical association declaration of Helsinki: ethical principles for medical research involving human subjects. *JAMA* 2013; 310: 2191–2194.
11. Lencioni R and Llovet JM. Modified RECIST (mRECIST) assessment for hepatocellular carcinoma. *Semin Liver Dis* 2010; 30: 52–60.
12. Hiraoka A, Kumada T, Kudo M, *et al.* Albumin-Bilirubin (ALBI) grade as part of the evidence-based clinical practice guideline for HCC of the Japan society of hepatology: a comparison with the liver damage and child-pugh classifications. *Liver Cancer* 2017; 6: 204–215.
13. Johnson PJ, Berhane S, Kagebayashi C, *et al.* Assessment of liver function in patients with hepatocellular carcinoma: a new evidence-based approach—the ALBI grade. *J Clin Oncol* 2015; 33: 550–558.
14. Eisen T, Joensuu H, Nathan PD, *et al.* Regorafenib for patients with previously untreated metastatic or unresectable renal-cell carcinoma: a single-group phase 2 trial. *Lancet Oncol* 2012; 13: 1055–1062.

15. Todesca P, Marzi L, Critelli RM, *et al.* Angiopoietin-2/Tie2 inhibition by regorafenib associates with striking response in a patient with aggressive hepatocellular carcinoma. *Hepatology* 2019; 70: 745–747.
16. Hayashi T, Yamashita T, Terashima T, *et al.* Serum cytokine profiles predict survival benefits in patients with advanced hepatocellular carcinoma treated with sorafenib: a retrospective cohort study. *BMC Cancer* 2017; 17: 870.
17. Lin J, Zhang Y, Wu J, *et al.* Neuropilin 1 (NRP1) is a novel tumor marker in hepatocellular carcinoma. *Clin Chim Acta* 2018; 485: 158–165.
18. Chan S, Chan A, Chan A, *et al.* Systematic evaluation of circulating inflammatory markers for hepatocellular carcinoma. *Liver Int* 2017; 37: 280–289.
19. Formenti S, Rudqvist N, Golden E, *et al.* Radiotherapy induces responses of lung cancer to CTLA-4 blockade. *Nature Med* 2018; 24: 1845–1851.
20. Lan Q, Peyvandi S, Duffey N, *et al.* Type I interferon/IRF7 axis instigates chemotherapy-induced immunological dormancy in breast cancer. *Oncogene* 2018; 38: 2814–2829.
21. Morimoto Y, Kishida T, Kotani SI, *et al.* Interferon-beta signal may up-regulate PD-L1 expression through IRF9-dependent and independent pathways in lung cancer cells. *Biochem Biophys Res Commun* 2018; 507: 330–336.
22. Hoshida Y. Nearest template prediction: a single-sample-based flexible class prediction with confidence assessment. *PLoS One* 2010; 5: e15543.
23. Hatanaka T, Kakizaki S, Nagashima T, *et al.* Analyses of objective response rate, progression-free survival, and adverse events in hepatocellular carcinoma patients treated with lenvatinib: a multicenter retrospective study. *Hepato Res*. Epub ahead of print 23 November 2019. DOI: 10.1111/hepr.13460.
24. Kodama K, Kawaoka T, Aikata H, *et al.* Comparison of clinical outcome of hepatic arterial infusion chemotherapy and sorafenib for advanced hepatocellular carcinoma according to macrovascular invasion and transcatheter arterial chemoembolization refractory status. *J Gastroenterol Hepatol* 2018; 33: 1780–1786.
25. Yin XM and Ding WX. Death receptor activation-induced hepatocyte apoptosis and liver injury. *Curr Mol Med* 2003; 3: 491–508.
26. Fullerton AM, Roth RA and Ganey PE. 2,3,7,8-TCDD enhances the sensitivity of mice to concanavalin A immune-mediated liver injury. *Toxicol Appl Pharmacol* 2013; 266: 317–327.
27. Rigamonti N, Kadioglu E, Keklikoglou I, *et al.* Role of angiopoietin-2 in adaptive tumor resistance to VEGF signaling blockade. *Cell Rep* 2014; 8: 696–706.
28. Berkkanoglu M, Guzeloglu-Kayisli O, Kayisli UA, *et al.* Regulation of Fas ligand expression by vascular endothelial growth factor in endometrial stromal cells in vitro. *Mol Hum Reprod* 2004; 10: 393–398.
29. Park-Windhol C and D'Amore PA. Disorders of vascular permeability. *Annu Rev Pathol* 2016; 11: 251–281.
30. De Lisi D, De Giorgi U, Lolli C, *et al.* Lenvatinib in the management of metastatic renal cell carcinoma: a promising combination therapy? *Expert Opin Drug Metab Toxicol* 2018; 14: 461–467.
31. Motzer RJ, Hutson TE, Glen H, *et al.* Lenvatinib, everolimus, and the combination in patients with metastatic renal cell carcinoma: a randomised, phase 2, open-label, multicentre trial. *Lancet Oncol* 2015; 16: 1473–1482.
32. Schlumberger M, Tahara M, Wirth LJ, *et al.* Lenvatinib versus placebo in radioiodine-refractory thyroid cancer. *N Engl J Med* 2015; 372: 621–630.
33. Ikeda K, Kudo M, Kawazoe S, *et al.* Phase 2 study of lenvatinib in patients with advanced hepatocellular carcinoma. *J Gastroenterol* 2017; 52: 512–519.
34. Yi M, Jiao D, Qin S, *et al.* Synergistic effect of immune checkpoint blockade and anti-angiogenesis in cancer treatment. *Mol Cancer* 2019; 18: 60.
35. Zhang G, Liu C, Bai H, *et al.* Combinatorial therapy of immune checkpoint and cancer pathways provides a novel perspective on ovarian cancer treatment. *Oncol Lett* 2019; 17: 2583–2591.
36. Hato T, Tabata M and Oike Y. The role of angiopoietin-like proteins in angiogenesis and metabolism. *Trends Cardiovasc Med* 2008; 18: 6–14.
37. Nie D, Zheng Q, Liu L, *et al.* Up-regulated of angiopoietin-like protein 4 predicts poor prognosis in cervical cancer. *J Cancer* 2019; 10: 1896–1901.
38. Argentiero A and De Summa S. Gene expression comparison between the lymph node-positive and -negative reveals a peculiar immune microenvironment signature and a theranostic role for WNT targeting in pancreatic ductal adenocarcinoma: a pilot study. *Cancers*. Epub ahead of print 4 July 2019. DOI: 10.3390/cancers11070942.